JOURNAL OF GEOPHYSICAL RESEARCH, VOL. 94, NO. D14, PAGES 16,437–16,448, NOVEMBER 30, 1989

Observations of Condensation Nuclei in the Airborne Antarctic Ozone Experiment: Implications for New Particle Formation and Polar Stratospheric Cloud Formation

J. C. WILSON,[1] M. LOEWENSTEIN,[2] D. W. FAHEY,[3] B. GARY,[4] S. D. SMITH,[5] K. K. KELLY,[3] G. V. FERRY,[2] AND K. R. CHAN[2]

The ER-2 Condensation Nucleus Counter (ER-2 CNC) was operated in the Airborne Antarctic Ozone Experiment in August, September, and October 1987. The ER-2 CNC measures the mixing ratio of particles, CN, with diameters from approximately 0.02 μm to approximately 1 μm. Comparisons of CN and other aerosol measurements with N_2O show that the vertical profile of the sulfate aerosol was probably displaced downward by the subsidence and mixing processes that determined the inclination of the N_2O isopleths. At altitudes above the minimum in the CN mixing ratio profile, CN mixing ratios correlated negatively with that of N_2O, demonstrating new particle production. The region of particle production was above and south of the 160 ppbv N_2O isopleth. The relationship between CN and N_2O did not change noticeably when moving from air containing normal levels of reactive nitrogen compounds (NO_y) to air depleted in those compounds. This suggests that the removal of NO_y was accompanied by the removal of a small minority of the CN. Concentrations of CN are compared with those of larger particles to study cloud formation mechanisms. In some cases condensation of water or nitric acid trihydrate following rapid cooling caused most of the CN to grow to diameters larger than 0.81 μm. Models published elsewhere predict that these conditions should result in a large fraction of particles growing to these sizes. Episodes of this type probably did not remove reactive nitrogen compounds through particle sedimentation from the chemically perturbed region. Small numbers of large particles were observed in other instances. The composition of the particles and their origins are unclear.

INTRODUCTION

Three interrelated populations dominate the stratospheric aerosol in the Antarctic winter and spring. These populations are the submicron sulfate particles, nitric acid trihydrate particles, and particles consisting mostly of water ice and, presumably, some nitric acid. These aerosols and their interactions are important in the processes which deplete ozone.

Satellite observations show that polar stratospheric clouds (PSCs) form in this region at low temperatures [*McCormick et al.*, 1989]. Models of aerosol growth [*Poole and McCormick*, 1988] show that the formation of nitric acid trihydrate ($HNO_3 \cdot 3H_2O$) particles and ice particles at low temperatures can explain important features observed in remote, optical measurements of PSCs. Nitric acid trihydrate particles with diameters near 1 μm, as well as larger particles, presumed to be mostly ice, have been observed in situ [*Fahey et al.*, 1989].

Reactions occurring on the surface of the predominantly ice particles may release chlorine [*Molina et al.*, 1987; *Tolbert et al.*, 1987], which destroys ozone. Removal of nitric acid from the gas phase is necessary for the maintenance of high concentrations of active chlorine and the catalytic destruction of ozone [*Solomon*, 1988]. It is widely thought that gravitational sedimentation of large particles containing nitric acid is responsible for its removal.

The sulfate particles are always present and serve as nuclei for PSC formation. Their size distribution depends upon altitude and likely affects the properties of the PSCs [*Poole and McCormick*, 1988; *Toon et al.*, 1989]. At midlatitudes the sulfate volume mixing ratio has a maximum near 20-km altitude, and the number mixing ratio profile has a minimum near the same location (D. J. Hofmann, Stratospheric sulfuric acid aersol background increase 1960–1988, submitted to *Nature*, 1988). In the spring, at high latitudes in the southern hemisphere, the maximum in volume and minimum in number occur at lower altitudes, and a particle production mechanism is observed at higher altitudes [*Hofmann et al.*, 1988].

The aerosol and gas measurements made from the ER-2 in the Airborne Antarctic Ozone Experiment (AAOE) of 1987 permit physical characteristics of the aerosol to be compared with dynamical and chemical tracers. This permits study of the processes affecting these populations and their interactions. This paper focuses on the results of the Er-2 Condensation Nucleus Counter (ER-2 CNC) which provides a measure of aerosol number mixing ratio. The aerosol number mixing ratio in an air parcel can be changed by new particle formation, by mixing with air having a different mixing ratio, by coagulation, or by cloud processes. If these processes are negligible, the mixing ratio remains constant under changes in pressure or temperature.

In this paper, the effect of subsidence in the polar region on the profile of aerosol number mixing ratio and on the sulfate aerosol is discussed. Evidence for new sulfate particle formation is presented and related to the amount of

[1]Department of Engineering, University of Denver, Colorado.
[2]NASA Ames Research Center, Moffett Field, California.
[3]Aeronomy Laboratory, National Oceanic and Atmospheric Administration, Boulder, Colorado.
[4]Jet Propulsion Laboratory, Pasadena, California.
[5]Dillon Smith Engineering, Inc., St. Louis Park, Minnesota.

Paper number 89JD01186.
0148-0227/89/89JD-01186$05.00

subsidence experienced by air parcels in the formation of the polar vortex. Measurements in air from which nitric acid has been removed are compared with measurements in air from which nitric acid has not been removed to determine the effect of this process on the sulfate aerosol number. The fraction of nuclei which have participated in clouds is determined and compared with existing theories.

DESCRIPTION OF INSTRUMENTS AND KEY MEASUREMENTS

ER-2 Condensation Nucleus Counter

The ER-2 CNC [*Wilson et al.*, 1983*a*] consists of a thermal growth chamber in which nuclei are grown to sizes which permit optical detection and an optical counter in which grown particles are individually counted. Sampling and transport systems bring the sample from the outside of the aircraft to the growth chamber and control the sample flow. The critical temperatures and flows are continuously monitored in flight so that correct instrument function is verified.

The continuous flow, thermal growth chamber in the ER-2 CNC consists of a saturator in which the aerosol sample is saturated with butyl alcohol vapor at 28°C followed by a condenser tube cooled to 5°C. In the condenser, the vapor becomes supersaturated, and the nuclei in the sample grow by condensation. Modeling of continuous flow growth chambers shows that the supersaturation for a given streamline in the flow depends upon the radial position of the streamline in the condenser [*Stolzenburg and McMurry*, 1986]. In the ER-2 CNC the aerosol sample is confined near the center streamline of the condenser so that all particles experience the same supersaturation. If the particle surface is wetted by the vapor, then this supersaturation determines the smallest particle which will grow. Experiments performed on the ER-2 CNC with particles of known size and concentration showed that at pressures between 53 and 187 mbar, more than 90% of all particles larger than 0.01 μm in diameter reaching the growth chamber are counted [*Wilson et al.*, 1983*a*].

The overall performance of the ER-2 CNC depends upon the characteristics of the sampling and transport system as well as those of the growth chamber and detector. Estimates of sampling efficiency were made based on assumptions concerning the fluid mechanics of the inlet. Transport efficiency was calculated from measured housekeeping variables.

Losses by diffusion were calculated using the results of Gormley and Kennedy [*Fuchs*, 1964]. Inertial losses of particles in the bends and losses by turbulent deposition were estimated using the results of *Chen and Wang* [1981] and *Pui et al.* [1987]. Effects of anisokinetic sampling were evaluated using the results of *Rader and Marple* [1988] for the three locations in the sampling and transport system where the sample is extracted from a larger flow. The analysis shows that the sampling efficiency should vary from 0.7 to 1.3 for particles in the 0.02- to 1-μm diameter range. However, comparisons with other aerosol sensors suggest that the ER-2 CNC lost particles having diameters near to and larger than 1 μm and that the upper size cutoff of the instrument is not well understood. It is likely that the CN measurements in some clouds in the AAOE underestimated the total number of particles present.

Definition of Condensation Nuclei

Condensation nuclei (CN) are the particles which are grown by condensation after creating a supersaturation in some working fluid, then counted. Usually these methods, reviewed by *Wilson et al.* [1983*a*], succeed in accurately measuring the aerosol number mixing ratio in the stratosphere, since the size range accurately counted by the instruments usually covers the size range present. The emphasis in CN counting has often been on the smallest particles detected by the instruments, since they are usually appreciably smaller than those typically detected by optical techniques. Therefore CN are often defined as the particles larger than the minimum size detected by the CNC. In the present case, the upper size cutoff of the instrument becomes important due to the occurrence of PSCs with mean diameters near 1 μm. Therefore, CN are defined here as particles in the 0.02- to 1-μm range. When the aerosol number distribution is dominated by particles outside of this range, the CN count provided by the ER-2 CNC may not accurately represent the total number of particles.

Potential Temperature

Potential temperature (θ) is defined in (1), where P is the ambient pressure in millibars and T is the temperature in degrees Kelvin.

$$\theta = T\left[\frac{1000}{P}\right]^{0.286} \tag{1}$$

Theta increases with altitude and is the vertical coordinate used most often in this discussion. Isentropic motion is along surfaces of constant θ. At high latitudes in winter, air cools diabatically by radiation. The sinking air parcels are said to be subsiding and cross surfaces of constant θ.

The FSSP

The FSSP is a laser aerosol spectrometer built by PMS, Inc., of Boulder, Colorado, and is operated by the NASA Ames Research Center [*Ferry et al.*, this issue]. The instrument sizes particles in the approximate diameter range from 0.81 to 9.74 μm.

The smallest size range in the FSSP data was found to be noisy, and 100 counts were subtracted from each 10-s FSSP count in this range. This correction was developed by *Fahey et al.* [1989] and corresponds to a subtraction of about 0.5 particles/cm^3. The uncertainty associated with this correction is of the same order of magnitude as the correction. A postmission calibration of the FSSP was done by *Baumgardner et al.* [1989], who also provide corrected channel boundaries. The corrections account for the differences between the refractive index of the calibration aerosol and of water and for the velocity dependence of the instrument response. Use of these boundaries is based on the assumption that the refractive index of the measured aerosol does not differ much from water. *Baumgardner et al.* [1989] also determined the size of the FSSP viewing volume and found the uncertainty in viewing volume to be ±45%.

The NO_y Instrument

The NO_y instrument measures reactive nitrogen compounds in both the aerosol and gas phase [*Fahey et al.*,

1989]. Gas phase species include NO, NO_2, NO_3, N_2O_5, HNO_3, $ClONO_2$, and HO_2NO_2. NO_y species on particles entering the instrument are released by evaporation and detected as equivalent gas phase NO_y. The instrument response to aerosol nitrate depends strongly on particle size because the inlet of the NO_y instrument is subisokinetic. Therefore the concentration of particles entering the inlet exceeds the population just upstream of the inlet. An external flow, inertial separator upstream of the NO_y inlet is designed to separate particles larger than about 5 μm from the air stream that impinges on the inlet of the NO_y instrument. The details of the separation efficiency as a function of particle size for the device are not certain. Nonetheless, NO_y on particles larger than the inertial cutoff size are not sampled.

Other Instruments

N_2O was measured with the ATLAS system described by *Loewenstein et al.* [1989]. The microwave temperature profiler (MTP), described by *Denning et al.* [this issue], permits mapping of the isentropic surfaces in the vicinity of the ER-2. When the plane is traveling parallel to the wind vector, the local temperature history of air parcels can be determined from the MTP data [*Gary*, 1989].

The ASAS-X is a laser aerosol spectrometer built by PMS in Boulder, Colorado, and operated by the NASA Ames Research Center. It is designed to measure the size and concentration of particles in the diameter range from 0.1 to 3 μm. During the transport of particles from the free stream to the laser cavity where the measurement is made, the aerosol is heated to temperatures well above ambient. It is likely that most of the nitric acid trihydrate or ice evaporates before the measurement. Thus the ASAS-X data are used here to describe the sulfate aerosol rather than PSC particles. Due to an instrument malfunction, a significant fraction of each sample was systematically undersized. Corrections for this systematic error have not been made; therefore the measured size distributions and magnitudes of derived quantities are not cited here. It is possible to account for these errors when making comparisons between ASAS-X measurements. In the uses of the ASAS-X data which follow, these errors have been taken into account. The output of the mass flow meter in the ASAS-X was used when calculating mixing ratios.

The total water instrument is described by *Kelly et al.* [1989]. The measurements of pressure, temperature, and location are described by *Chan et al.* [1989].

Units

The mixing ratio of CN is expressed as number of particles per milligram of air. Aerosol volume mixing ratios are expressed as μm^3 per milligram of air. Mixing ratios of gases are expressed as pptv, ppbv, or ppmv. These units represent one molecule of the species for every 10^{12}, 10^9, or 10^6 molecules of air, respectively.

Description of the Experiment

The AAOE is described in detail elsewhere [*Tuck et al.*, 1989]. Those features of AAOE relevant to this paper are highlighted here. The NASA ER-2 aircraft flew to Punta Arenas, Chile (latitude −53°), from NASA Ames Research Center (latitude 37°), via Panama and Puerto Montt, Chile (latitude −41°). Twelve missions were flown from Punta Arenas south toward Antarctica near the Palmer Peninsula between August 17 and September 22, 1987. Data were also taken on the ferry legs as the aircraft returned to Moffett Field. Figure 1 shows the potential temperature encountered along typical flight paths as a function of latitude. Most of the flights south from Punta Arenas were flown on surfaces of nearly constant potential temperature. The θ surfaces at about 425 and 455 K were frequently flown. At the south end of the flight path, a vertical profile was often flown.

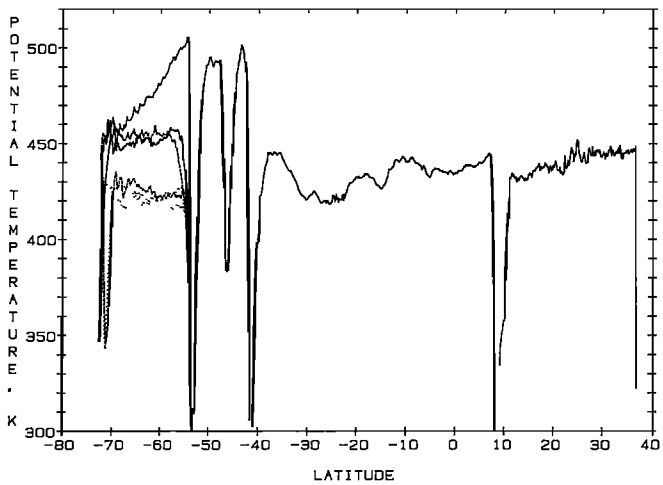

Fig. 1. Potential temperature as a function of latitude for return AAOE ferry flights and selected science flights: August 28 (dotted line), September 20 (solid line), and September 28 (dashed line).

Figure 2 shows the relationship between pressure altitude and θ for several flights south from Punta Arenas. In the southern portion of the flights, the geometric altitude may be as much as 2 km less than the pressure altitude, since the actual temperature profiles differ from those in the Standard Atmosphere.

A chemically perturbed region was encountered on flights

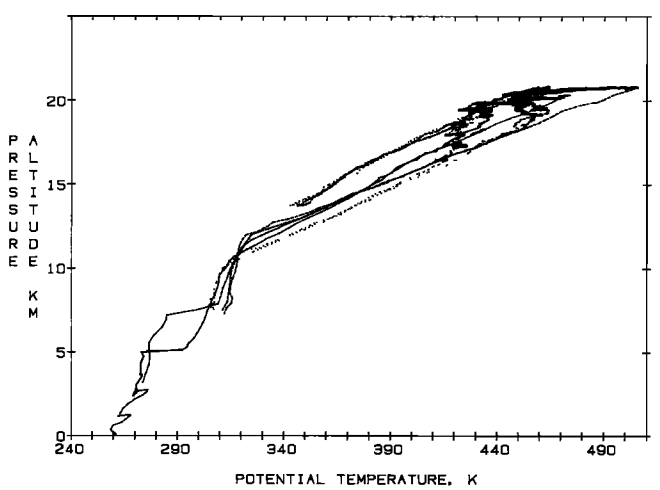

Fig. 2. Pressure altitude as a function of potential temperature for three flights. The pressure altitudes do not accurately represent geometric altitudes due to the temperature structure of the atmosphere. August 28 (dotted line), September 20 (solid line), and September 28 (dashed line).

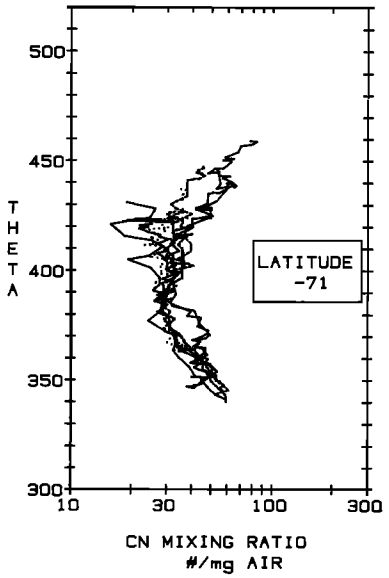

Fig. 3. Mixing ratio profiles measured at −71° latitude on four days: August 28 (solid line), August 30 (dotted line), September 9 (dashed line), and September 20 (solid line). The September 20 profiles reach highest potential temperatures.

south from Punta Arenas [*Proffitt et al.*, 1989]. At latitudes which varied from flight to flight, but averaged −65.6°, an abrupt increase in chlorine monoxide, ClO, was noted. This was often accompanied by decreases in water and NO_y. It is generally believed that water and NO_y were removed from the sampled air parcels through the sedimentation of large aerosol particles consisting mainly of ice and nitrates. Increasingly with time, ozone was seen to decrease in the chemically perturbed region (CPR). For the purposes of the discussion which follows, the edge of this region is arbitrarily defined as that point at which the ClO mixing ratio reaches 130 pptv. This point is referred to below as the ClO wall. Due to the paths flown, this feature was encountered within two potential temperature ranges: from about 415 K to about 430 K and from about 445 K to about 460 K.

The ER-2 CNC acquired data on 11 of the 12 flights south from Punta Arenas, failing on August 23. The instrument acquired data on four of the ferry legs, including all three of the return legs. On September 21 the ER-2 CNC measured mixing ratios which were a factor of 2 smaller than values seen on September 20 and 22. The exclusion of the September 21 data from the figures below is based on subjective judgment.

Features of the N_2O Measurement and Definition of NO_y^*

N_2O is a long-lived tracer for tropospheric air, since its source is in the troposphere and it is destroyed in the stratosphere. The mixing ratio of N_2O generally decreases with increasing altitude and θ. Since the lifetime of N_2O is long compared with the processes which perturb the chemistry in the polar vortex, it serves as a dynamical tracer which indicates origins of air parcels. When comparing air parcels, the ones with smaller mixing ratios of N_2O are likely to have come from higher in the stratosphere or to have been there longer. Parcels with larger mixing ratios of N_2O show more influence of the troposphere. In AAOE, N_2O was observed to decrease on surfaces of constant θ while moving south from Punta Arenas. *Podolske et al.* [this issue] draw several conclusions from these observations: that the air in the region was not well mixed meridionally, that a gradient in subsidence occurred during the winter, with greater subsidence occurring poleward, and that the air sampled at the south end of the flights subsided by 3–5 km more than that over Punta Arenas. Although north-south mixing was not complete, *Podolske et al.* [this issue] conclude that the location of the N_2O isopleths was determined by a combination of mixing along θ surfaces and subsidence.

Fahey et al. [1989, this issue] developed a means of estimating the amount of NO_y which was originally in an air parcel from the N_2O mixing ratio. This expected amount of NO_y is referred to as NO_y^*. When the mixing ratio of NO_y^* exceeds the measured NO_y, NO_y has been removed from the parcel or is on particles which were separated from the NO_y instrument inlet by the inertial separator. When NO_y exceeds NO_y^*, the NO_y signal includes aerosols being sampled and enhanced in the NO_y inlet. The term denitrification denotes either partial or total removal of NO_y from an air parcel.

GEOGRAPHICAL DISTRIBUTION OF CN AND RELATION TO N_2O

Observations of Geographical Distribution of CN

Figure 3 shows vertical profiles measured at latitudes near −71. These profiles were located from 1° to 10° latitude south of the ClO wall and are all in the CPR. Most of the profiles measured in this region show a mixing ratio minimum at a value of θ between 380 and 420 K. The ASAS-X data indicate that the sulfate aerosol volume mixing ratio profile has a maximum at the same θ as the CN minimum.

Figure 4 shows typical vertical profiles of CN mixing ratio

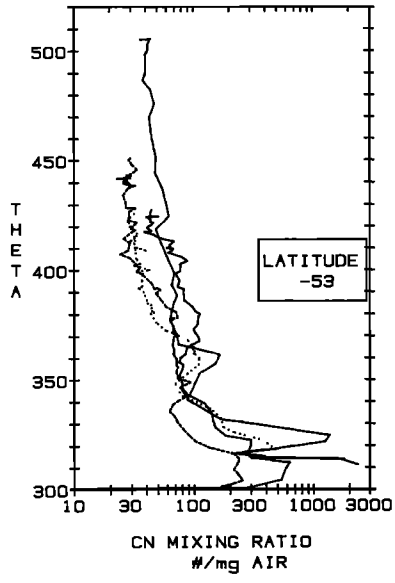

Fig. 4. Mixing ratio profiles measured at −53° latitude on four days: August 28 (solid line), August 30 (dotted line), September 9 (dashed line), and September 20 (solid line). The September 20 profiles reach highest potential temperatures.

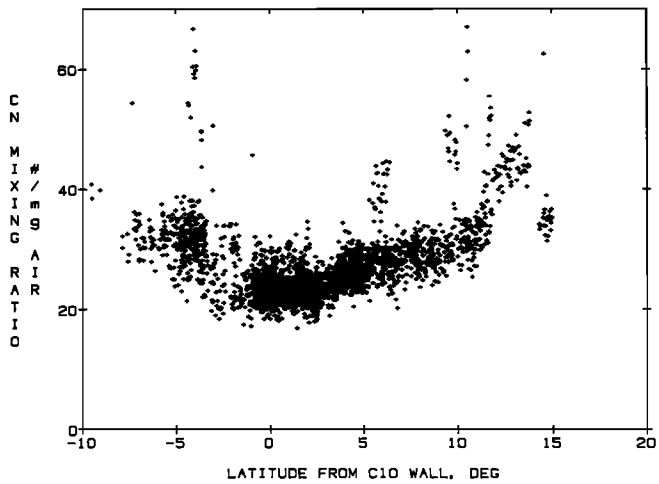

Fig. 5. CN mixing ratio as a function of latitude from the ClO wall for θ between 422 and 427 K. All flights except September 21 are plotted.

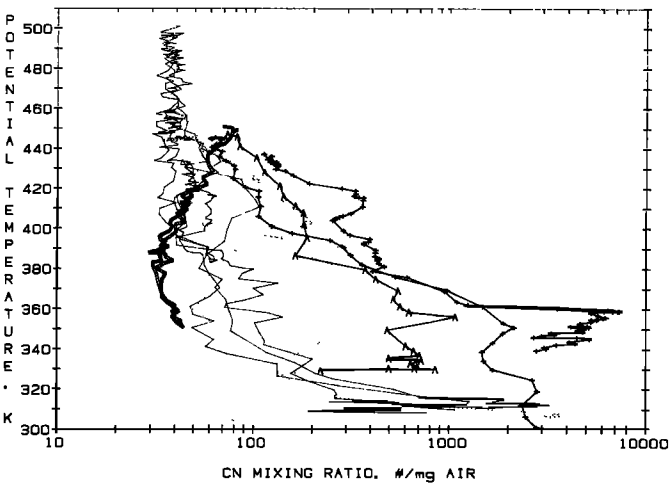

Fig. 7. Mixing ratio as a function of potential temperature. Panama (plus signs), Moffett Field, California (A), Puerto Montt, Chile (dotted line), Punta Arenas, Chile (solid line), and latitude −72° (double solid line).

measured near −53° latitude. Mixing ratios generally decrease as θ increases above 300 K. Those profiles reaching $\theta > 450$ K usually have a region of nearly constant CN mixing ratio extending from the top end of the decreasing segment to the top of the profile. On average, the lower edge of this CN plateau is found at $\theta = 440$ K. The highest θ reached in these profiles was about 505 K. The ASAS-X shows that the sulfate aerosol volume mixing ratio tends to correlate negatively with CN on these profiles. Sulfate volume generally increases as CN decreases above θ of 300 K and shows a plateau with a maximum value where CN has a plateau with a minimum.

Figure 5 shows mixing ratios measured between 422 and 427 K as a function of latitude from the ClO wall. The range of θ has been restricted to emphasize the latitudinal dependence. The mixing ratio increases to the south of the ClO wall and decreases south from Punta Arenas to a minimum just north of the ClO wall. Figure 6 shows a similar plot for values of $\theta \sim 455$ K. In this plot the mixing ratio increases south of the ClO wall.

CN mixing ratio profiles in the CPR, near Punta Arenas, and at various locations in the ferry flights are shown in Figure 7. For the most part, smaller mixing ratios were observed near Punta Arenas and in the CPR than in the tropics and northern hemisphere mid-latitudes.

Relation Between CN and N_2O Mixing Ratios

CN mixing ratios showed both positive and negative correlations with N_2O during the AAOE study. Figure 8 shows a scatter plot of CN mixing ratio against N_2O for 11 flights between August 28 and October 3. All the available data from −71° to about 35° are plotted. CN tend to be positively correlated with N_2O for N_2O values larger than about 160 ppbv. For mixing ratios of N_2O less than 150 ppbv, CN mixing ratios tend to correlate negatively with the N_2O mixing ratios. Most locations where N_2O mixing ratios exceeded 240 ppbv were north of Punta Arenas, and those where N_2O was less than 130 ppbv were south of Punta

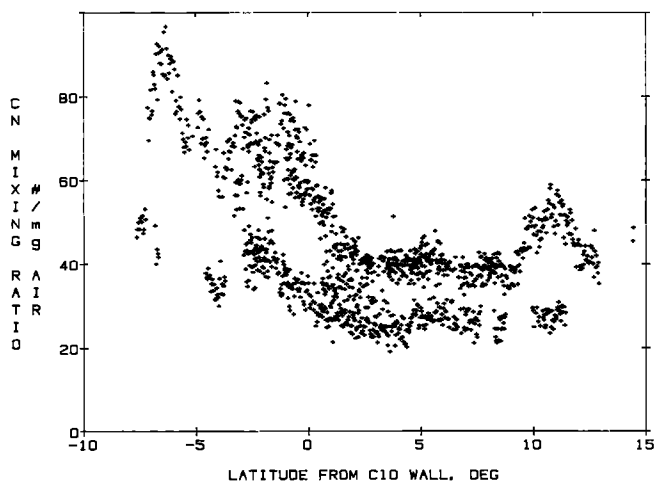

Fig. 6. CN mixing ratio as a function of latitude from the ClO wall for θ between 450 and 460 K. All flights except September 21 are plotted.

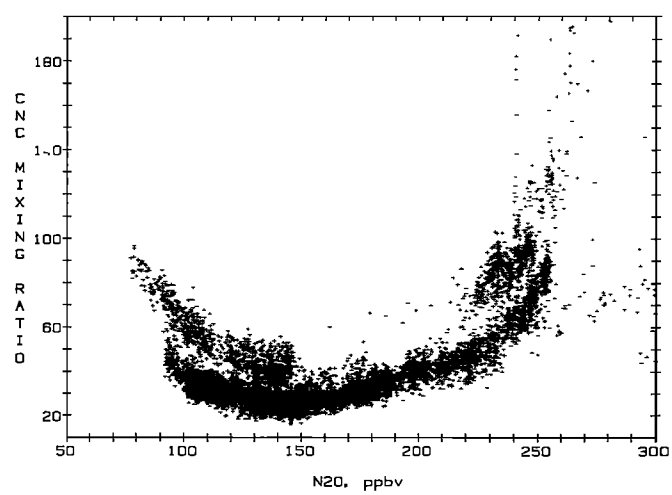

Fig. 8. CN mixing ratio plotted as a function of N_2O mixing ratios. All flights included except September 21.

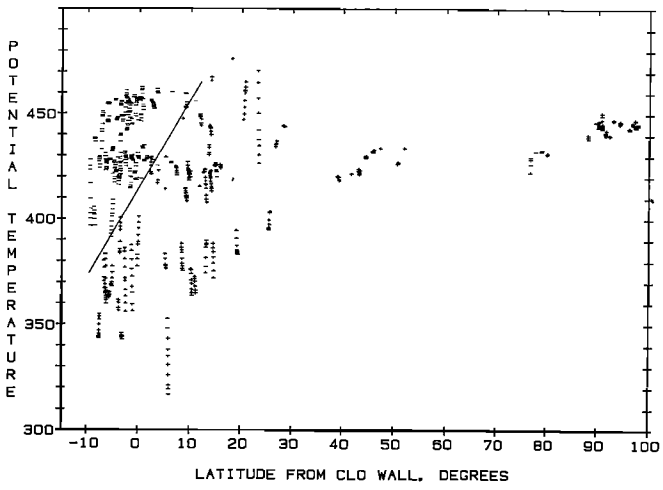

Fig. 9. Locations where correlations between CN and N_2O exceed +0.5 or are less than −0.5. Correlations were calculated over 400-s intervals using 20 data points. Each data point used in the correlation was an average over 20 s. The solid line indicates a boundary between positive and negative correlations. The horizontal axis is latitude from the ClO wall as determined for each flight.

Arenas. Sorting into narrow bins in θ or temperature did not reduce the scatter in the CN-N_2O data.

Figure 9 shows the geographical distribution of the sign of the CN-N_2O correlation. Each correlation was calculated with 20 pairs of points measured along approximately 80 km of flight path. Each of the 20 points is an average over twenty 1-Hz measurements. A moving correlation was done. Locations where the CN-N_2O correlation exceeds 0.5 are indicated with a plus sign, and locations where it is less than −0.5 are indicated with a minus sign. Most of the points above the sloped dividing line are negative, and most below and to the right are positive. *Podolske et al.* [this issue] present a contour plot of the N_2O mixing ratio on potential temperature-latitude coordinates. The dividing line in Figure 9 falls very near the 160 ppbv isopleth in their contour plot. Air above and south of the dividing line has N_2O mixing ratios less than 160 ppbv, and air to the north and below it has N_2O mixing ratios greater than 160 ppbv.

Discussion of CN Distribution

For N_2O mixing ratios in excess of about 160 ppbv, CN and N_2O correlate positively. The vertical CN mixing ratio profiles in Figures 3 and 4 show this effect where CN is increasing as θ decreases. This is likely due to the increasing influence of tropospheric air as N_2O increases. The troposphere is a source of both CN and N_2O.

For N_2O mixing ratios less than about 150 ppbv, CN and N_2O correlate negatively. Since decreasing N_2O indicates increasing influence of stratospheric air, this negative correlation shows the effect of a high-altitude source of CN. Increasing CN mixing ratios with increasing θ illustrate a region where this occurs in Figure 3.

The dividing line in Figure 9 was drawn to separate regions of positive and negative correlation between CN and N_2O. Figure 8 shows that the minimum in CN mixing ratio falls between these regions of positive and negative correlation. Therefore the dividing line also indicates the approximate location of the minimum in the CN mixing ratio vertical profiles.

Since the dividing line in Figure 9 falls very near the 160-ppbv N_2O isopleth, Figure 9 associates the location of the minimum in the CN mixing ratio profile with a narrow range of N_2O mixing ratios, as does Figure 8. In the absence of subsidence, isopleths of N_2O should be parallel to surfaces of constant θ [*Loewenstein et al.*, 1989]. Therefore in the early months of 1987 prior to the setup of the polar vortex and CPR, it is likely that the CN vertical profiles were similar in the −53°–−71° region. That is, the mixing ratios of CN probably decreased as θ increased to values above 440 K and were nearly constant above that to $\theta > 500$ K. Later in the season, subsidence and mixing on θ surfaces established the slope of the N_2O isopleths. The CN profile subsided with the air. The line connecting the points where CN mixing ratio profiles stopped decreasing with θ acquired the same inclination as the N_2O isopleths. Above this line, particle production (discussed below) occurred, and the line became the locus of the minima in the CN profiles.

The flight segments at nearly constant θ showed structure which is consistent with differential subsidence of a fairly uniform profile. Figure 5 shows that the CN mixing ratio was often observed to decrease south of Punta Arenas at $\theta \sim 425$ K. The profiles at −53° often continued to decrease at $\theta >$ 425 K. Increasing subsidence poleward brought those lower values of CN mixing ratio to the 425 K surface south of Punta Arenas. The increase in CN mixing ratio south of the ClO wall resulted from the increased subsidence experienced at those locations, causing the high-altitude source to exert more influence.

The number and volume mixing ratios indicated by the ASAS-X are consistent with the interpretation of the CN data. The maximum in sulfate aerosol volume mixing ratio is found at the same θ as the minimum in CN, as would be expected following subsidence. Sulfate filter sulfate measurements [*Gandrud et al.*, 1989] also show decreasing mass mixing ratios as the ER-2 proceeded south on surfaces of constant θ. Differential subsidence turned a gradient in altitude into one in latitude with the result that the filter samples were taken at altitudes increasingly above the maximum in mass mixing ratio in the sulfate layer. At −71° the filter sulfate mass mixing ratios often increased as the ER-2 descended to lower altitudes and toward the maximum in the sulfate mass mixing ratio profile.

Loewenstein et al. [1989] argue that the subsidence occurred prior to the start of AAOE. The effect of the subsidence on the sulfate aerosol size distribution at any fixed geometric altitude can be inferred from the CN and ASAS-X profile data. At altitudes above the CN minimum, the sinking air likely brought smaller volume mixing ratios and constant or increasing CN mixing ratios to a given geometric altitude. Thus the size distribution shifted toward smaller sizes. This shift affected the optical properties of the aerosol observed in the absence of clouds. The ER-2 aerosol data suggest that the scattering ratio at a given geometric altitude should have decreased with time as the CN minimum sank below it. The scattering ratio data [*McCormick et al.*, 1989] do show a decrease at the appropriate altitudes during the time of the subsidence. It is also likely that during the subsidence the size distribution of the PSC nuclei and the microphysics of PSC formation changed with time at fixed geometric altitudes.

CN profiles were measured at −78° with the balloon-borne University of Wyoming CNC [*Hofmann et al.*, 1989] and show minima in mixing ratios at potential temperatures near 385 K. The mixing ratios reported at −78° on August 29 were roughly twice the values reported for the minima measured by the ER-2 CNC at −71°. It is expected that the CN mixing ratio minimum would occur at smaller values of θ at higher latitudes than it does at −71°, since more subsidence should have occurred at higher latitudes. The increase in the minimum CN mixing ratio observed at −78° may be partially due to the increased effect of the upper altitude source due to increased subsidence.

NEW PARTICLE FORMATION

Background

Observations of new particle formation in the stratosphere have been attributed to either chemical or thermal mechanisms. The first involves gas phase reactions between sulfur-bearing gases and free radicals producing sulfuric acid vapor, which can condense to produce particles [*Turco et al.*, 1982; *McKeen et al.*, 1984]. Examples of chemical production of new particles in the presence of preexisting aerosol were observed following volcanic eruptions when large amounts of SO_2 were injected into the stratosphere [*Hofmann and Rosen*, 1981; *Wilson et al.*, 1983*b*].

The thermal mechanism involves the evaporation and recondensation of sulfuric acid and was observed at mid-latitudes following sudden warmings in polar regions which presumably vaporize sulfuric acid particles. Subsequent transport of the vapor to cooler regions led to high levels of supersaturation, and nucleation resulted [*Hofmann et al.*, 1985]. These events enhanced mixing ratios by orders of magnitude in the 25- to 30-km altitude range following warmings. *Hofmann et al.* [1985] suggest that this mechanism causes an apparently global layer of CN in this altitude range. This layer appears in balloon soundings, which reveal a minimum in the CN mixing ratio at altitudes of 18–22 km (D. J. Hofmann, Stratospheric sulfuric acid aerosol background increase 1960–1988, submitted to *Nature*, 1988) and an increase in mixing ratio at higher altitudes. This thermal source may also explain the observed reversals of correlation between CN and O_3 in mid-latitudes at pressure altitudes of 20 km near the jet stream (J. C. Wilson et al., Measurements of condensation nuclei above the jet stream: Evidence for cross jet transport by waves and new particle formation at high altitudes, submitted to *Journal of Geophysical Research*, 1989.) At lower altitudes, a negative correlation between CN and O_3 indicates a tropospheric source for the CN.

Balloon-borne CN measurements in the Antarctic spring of 1986 revealed a layer of greatly enhanced CN above the region of ozone depletion [*Hofmann et al.*, 1988]. Both thermal and chemical mechanisms have been suggested to explain this CN layer.

Oppenheimer [1987] suggested that the CN layer might have been formed from the products of oxidation of OCS by OH. His calculations show that typical stratospheric concentrations of OCS and the enhanced concentrations of OH suggested by *Crutzen and Arnold* [1986] would produce the required particles in 1–2 months. These workers argue that enhanced OH concentration is a likely result of denitrification and is another way in which the Antarctic vortex is chemically perturbed.

Hofmann et al. [1988] suggest that subsiding air and radiative cooling could result in high sulfuric acid vapor supersaturations. The sulfuric acid vapor concentration increases with altitude, and subsidence is likely to increase the saturation. This could be followed by homogeneous and/or ion nucleation and the creation of new particles without requiring additional sulfuric acid production via chemical mechanisms.

New Particle Formation Observations in AAOE

The negative correlation between mixing ratios of CN and N_2O shown in Figures 8 and 9 demonstrates the effects of a source of CN at altitudes above the minimum in the CN vertical profile. Due to the lifetime of CN, it is not possible to know whether the production occurred during or before AAOE. The negative correlations were observed in AAOE whenever sufficiently low N_2O mixing ratios were encountered. Thus a starting date for this particle production cannot be inferred from the AAOE data.

Increases in CN at low mixing ratios of N_2O are not matched by increases in the ASAS-X signal. Since the ASAS-X detects particles larger than about 0.1 μm, it is likely that the newly produced particles are smaller than 0.1 μm. It is also likely that these new particles are not volatile, since they survive heating to 28°C in the saturator of the ER-2 CNC. Thus the counted particles probably consist of $H_2SO_4 \cdot nH_2O$, since both pure $HNO_3 \cdot 3H_2O$ and H_2O should evaporate in the ER-2 CNC saturator.

Discussion of New Particle Formation

The observations of new particle formation discussed here do not rule out either chemical production of sulfuric acid vapor or an increase in the saturation of existing vapor due to subsidence.

Support for thermal formation of new particles in subsiding air parcels comes from the correlation between observed new particles and N_2O mixing ratios. Air parcels with the low N_2O mixing ratios probably subsided more than parcels with high mixing ratios and generally have more particles. The thermal explanation for the particles suggests that greater subsidence would cause greater increase in the saturation of sulfuric acid vapor and would make a greater quantity of vapor available.

The new particles correlate more closely with the dynamical tracer, N_2O, than with any of the chemical tracers associated with the CPR, such as ClO or denitrification. For example on September 22, CN was negatively correlated with N_2O north of the ClO wall at $\theta \sim 450$ K, where denitrification had not occurred. Figure 9 shows a number of occurrences this type north of the ClO wall. Also, the boundary of the region in which new particles were observed is parallel to isopleths of N_2O and is inclined with respect to the boundary of the chemically perturbed region. The boundary of the chemically perturbed region was only located and defined for values of θ near 425 and 455 K.

It is not known if there is sufficient sulfuric acid vapor at the appropriate altitudes to form the particles observed after subsidence of 3–5 km. However, if the new particles are

assumed to have diameters near the low end of the detectable size range and little vapor is assumed to condense on preexisting particles, the sulfuric acid vapor vertical profiles measured by *Arnold et al.* [1981] provide just enough sulfuric acid to account for the new particles.

The production of CN observed outside of the chemically perturbed region does not rule out a chemical origin for the new particles. CN usually have long lifetimes compared with ClO. Therefore it is possible that particles could have been formed in parcels containing elevated OH and ClO and that the ClO disappeared later. This could happen if NO_y were deposited on PSC particles which were too small to sediment significantly. Then the perturbed chemistry would disappear after the evaporation of the PSC. New particles made while the chemistry was perturbed would exist longer than the indications of the perturbed chemistry which caused them.

A second chemical mechanism can be suggested in addition to that of *Oppenheimer* [1987]. Rates and products of reactions between ClO and OCS are not known. However, the upper limits for these reactions [*DeMore et al.*, 1987] and reasonable concentrations for OCS [*Oppenheimer*, 1987] together with the measured values of ClO concentration do not preclude the possibility that the new particles were formed from products of oxidation of OCS by ClO. In such an instance, the formation of the new particles would not serve as a significant sink for ClO, since the numbers of reacting molecules would be small compared with the measured ClO concentrations.

The number of particles produced is affected by the quantity of preexisting aerosol as well as the saturation and properties of the condensing vapor. Preexisting aerosol provides a surface on which the vapor condenses, and this condensation competes with new particle formation. The dividing line in Figure 9 identifies the approximate location of the minimum in the CN mixing ratio profiles and the maximum in aerosol volume mixing ratio. It is likely that the quantity of preexisting aerosol surface also decreases to the south and above the dividing line. If so, this would facilitate the increased formation of new particles which is observed when moving to the south and above the line. The aerosol size distribution in this region is likely to be bimodal. The new particles will probably form a mode with a diameter small compared with that of the preexisting aerosol.

The relationship between the increases in CN reported here and the layer of CN reported at −78° [*Hofmann et al.*, 1989] is unknown. It is worth noting that this layer seems to be formed in a region having very little preexisting aerosol.

CN Mixing Ratios in and out of Denitrified Air

Observations

Figure 10 is a plot of CN versus N_2O for denitrified and nondenitrified air on September 22. Nitrate aerosols are not present on this day. Therefore air in which NO_y is significantly less than NO_y^* has been denitrified. Data in the figure are sorted into two groups: those points for which $NO_y/NO_y^* < 0.25$ represent denitrified air, and points for which $NO_y/NO_y^* > 0.75$ represents air which is not significantly denitrified. The points with $N_2O > 120$ ppbv and $NO_y/NO_y^* < 0.25$ were encountered in the profile near −71°. For values of N_2O between 140 and 190 ppbv, the CN mixing ratio is

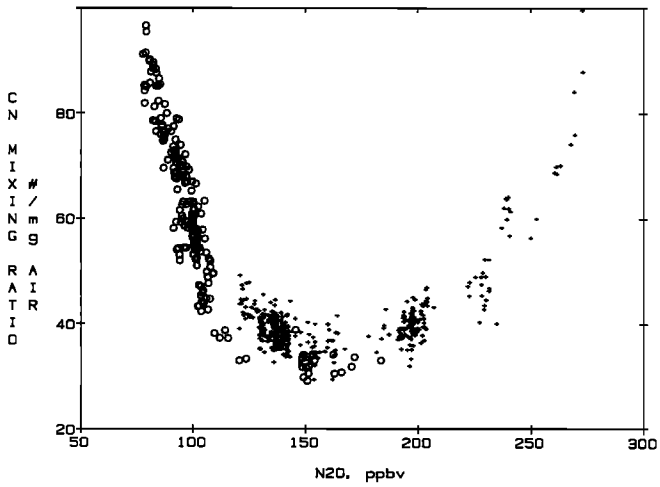

Fig. 10. CN mixing ratio plotted as a function of N_2O for September 22, 1987. Data are segregated into two classes. For the data indicated with plus signs, NO_y/NO_y^* exceeds 0.75. These points represent air which is not significantly denitrified. The points marked with open circles have values of NOy/NO_y^* less than 0.25 and represent denitrified air.

approximately 15% less in denitrified air than in nondenitrified air. On September 16 the denitrified air holds slightly more CN. So within approximately ±20%, CN mixing ratios are the same in denitrified and nondenitrified air having the same N_2O mixing ratios.

Implications for Removal of NO_y

Comparison of these different air parcels requires some justification. The nondenitrified air parcels with $N_2O \sim 150$ ppbv were found north of the ClO wall at $\theta > 415$ K. The denitrified parcels with similar N_2O mixing ratios were found south of the ClO wall at $\theta < 400$ K. If the differential subsidence scenario described above is correct, then it is reasonable to assume that the parcels were at similar potential temperatures and contained similar aerosols before the chemically perturbed region was established.

The comparison of denitrified and nondenitrified air suggests that the removal of NO_y was accompanied by removal of only 0–20% of the CN. If a significantly greater fraction of CN were removed, the comparison requires that the particle production process replaced most of them. It is likely that the larger particles in the sulfate distribution would serve as nuclei for PSCs and hence be removed. If a significant fraction of them were removed and were replaced by smaller, newly formed ones, the size distribution of the aerosol would shift to smaller sizes. Signs of this shift are not seen in the ASAS-X data. Thus, if the replacement occurred, the new small particles had to grow by condensation of gas phase sulfuric acid, so that the final distribution resembled the initial one. A significant amount of sulfate would have been required. At these altitudes there is probably not enough sulfuric acid vapor in the air mass to replace a significant fraction of the sulfate aerosol [*Arnold et al.*, 1981], and the conversion of OCS to sulfuric acid vapor is probably too slow to provide the required sulfate [*Oppenheimer*, 1987].

The limitations of the ASAS-X data and the uncertainties concerning available sulfate weaken the argument against the removal of a significant fraction of the CN. But the

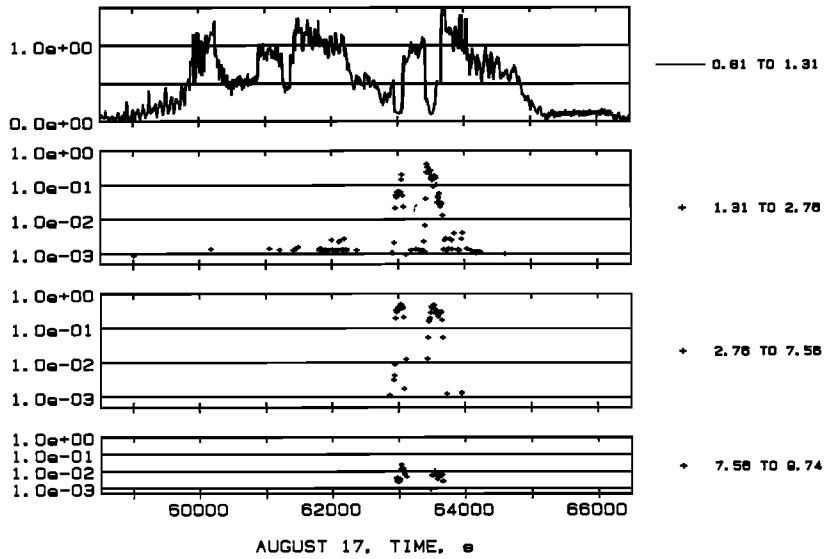

Fig. 11. Fraction of total particles measured in each size range on August 17. The bottom three curves are shown with a log scale. From top to bottom the diameter ranges are 0.81–1.31, 1.31–2.76, 2.76–7.56, and 7.56–9.74 μm.

comparison constrains the aerosol processes, requiring removed aerosol to be replaced.

Comparison of CN and Larger Particles in PSC Formation

Background

The formation of aerosols containing nitric acid was predicted by *Crutzen and Arnold* [1986], *Toon et al.* [1986], and *McElroy et al.* [1986] and confirmed by *Fahey et al.* [1989], *Gandrud et al.* [1989], and *Pueschel et al.* [1989]. The measurements of *Hanson and Mauersberger* [1988] show that nitric acid trihydrate ($HNO_3 \cdot 3H_2O$) will form at temperatures and water and nitric acid concentrations frequently occurring in the polar vortex. The temperatures are above those needed to form ice particles. The $HNO_3 \cdot 3H_2O$ particles can serve as a removal mechanism if they are large enough. Small particles settle too slowly to be removed and may sublimate, releasing nitric acid. Removal of nitric acid from the gas phase is necessary for the maintenance of high concentrations of active chlorine and consequent destruction of ozone [*Solomon*, 1988]. *Fahey et al.* [this issue] show that up to 90% or ~ 10 ppbv of NO_y has been removed from the CPR.

It is known that PSC particles which are predominantly ice can serve as sites for heterogeneous reactions necessary for the release of active chlorine [*Molina et al.*, 1987]. Although removal of water by sedimenting ice particles may not be necessary for ozone depletion, measurements of water vapor in the chemically disturbed region shows that it does occur [*Kelly et al.*, 1989].

Observations

Comparisons of concentrations of CN with concentrations of particles having diameters between 0.81 and 9.75 μm show that a variety of size distributions was observed in AAOE. In most cases when large particles were observed at operating altitudes, measured NO_y exceeded the mixing ratio of HNO_3 required to achieve saturation over $HNO_3 \cdot 3H_2O$. The mixing ratio of HNO_3 required to achieve saturation over $HNO_3 \cdot 3H_2O$ was calculated from the results of *Hanson and Mauersberger* [1988], the temperature, and water vapor concentration. At these times, it was possible that particles of $HNO_3 \cdot 3H_2O$ were in equilibrium with water and nitric acid vapor. But saturation is not assured, since NO_y includes more than nitric acid. Occasions when water vapor was found to be saturated with respect to ice were also examined.

Plots of the fraction of particles having grown into specific size ranges are presented in Figures 11–13 for August 17, 18, and 30. The plotted data contain most of the episodes encountered at operating altitudes during which the FSSP indicated significant aerosol volume and for which CN and NO_y data are available. These observations are typical of those made on other days for which the data set was not complete.

The total mixing ratio of particles present is determined by adding the CN mixing ratio to the mixing ratio of particles with diameters larger than 1.06 μm measured by the FSSP. The FSSP data provide the mixing ratio in each size range. The uncertainty in the upper size limit of the ER-2 CNC and the uncertainty in the FSSP viewing volume may account for the occurrence of fractions as large as 1.5.

On August 17, water mixing ratios exceed that necessary for saturation over ice at times near 63,000 and 63,500 s. The resulting size distribution (referred to as SD1) is characterized by a large fraction of the particles having grown to diameters larger than 1.31 μm. While fewer than 10% grew to diameters between 7.56 and 9.47 μm, the majority of the particles grew to larger than 2.76 μm in diameter.

A second type of size distribution (SD2) has a significant fraction of the total aerosol number in the 0.81- to 1.31-μm range. When SD2 was present, the FSSP signal in this size range correlated with the NO_y signal, indicating that these particles contained NO_y. The population of larger particles in SD2 is less than a few per thousand. SD2 occurred over much of the interval between 60,000 and 65,000 s on August 17, except during the ice events. On August 18, SD2 was

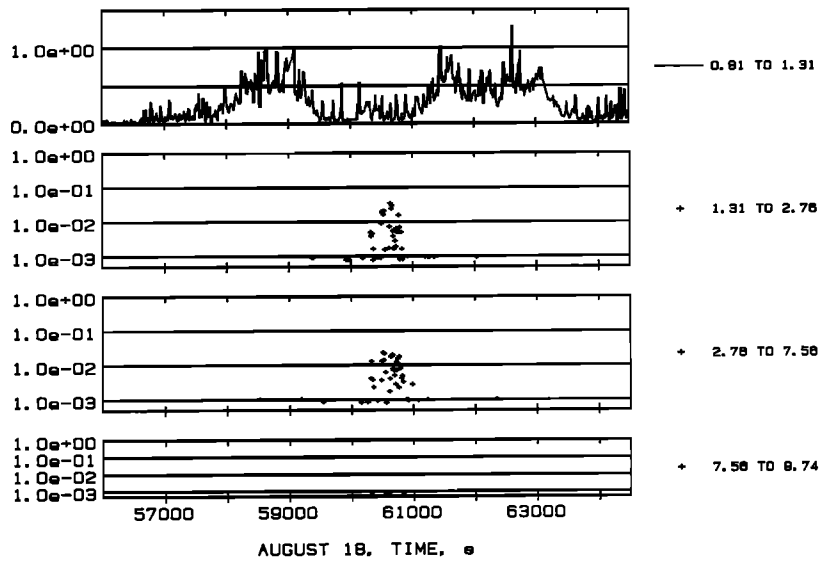

Fig. 12. Fraction of total particles measured in each size range on August 18. The bottom three curves are shown with a log scale. From top to bottom the diameter ranges are 0.81–1.31, 1.31–2.76, 2.76–7.56, and 7.56–9.74 μm.

observed from about 58,200 to 59,200 s and from about 61,300 to 63,100 s. On August 30, time intervals from 57,500 to 58,000 s, from about 59,700 to 60,200 s, and around 61,500 and 62,500 s all show positive correlations between NO_y and the fraction of particles in the range 0.81–1.31 μm. For the most part, these intervals on August 30 show evidence of denitrification. That is, NO_y is less than NO_y^*. Yet there appear to be particles in the 0.81- to 1.31-μm range containing NO_y.

A third type of size distribution (SD3) is seen between 60,000 and 61,000 s on August 18 and around 57,000 and 63,000 s on August 30. In these cases, large particles appear when there is minimal activity in the 0.81- to 1.31-μm range. These particles are not positively correlated with the NO_y signal. So either they did not contain significant quantities of NO_y or they did not reach the NO_y inlet. They occurred when mixing ratios of water vapor were less than required for saturation over ice, so they were not pure ice particles in equilibrium with ambient water vapor. These particles did occur when NO_y was less than NO_y^*. So they could have contained NO_y without causing the air parcel to contain more NO_y than would be predicted from the N_2O-NO_y correlation.

Discussion

The occurrence of ice particles observed on August 17 in the SD1 episodes seems to be well understood. Analysis of the Microwave Temperature Profiler and wind data shows that these events followed cooling in mountain waves and that a cooling rate of 0.011 K s^{-1} would be achieved in an air parcel following the isentropic surfaces through the mountain wave. This event was modeled by *Toon et al.* [1989], who used a cooling rate of 0.003 K s^{-1}. Toon et al.'s model

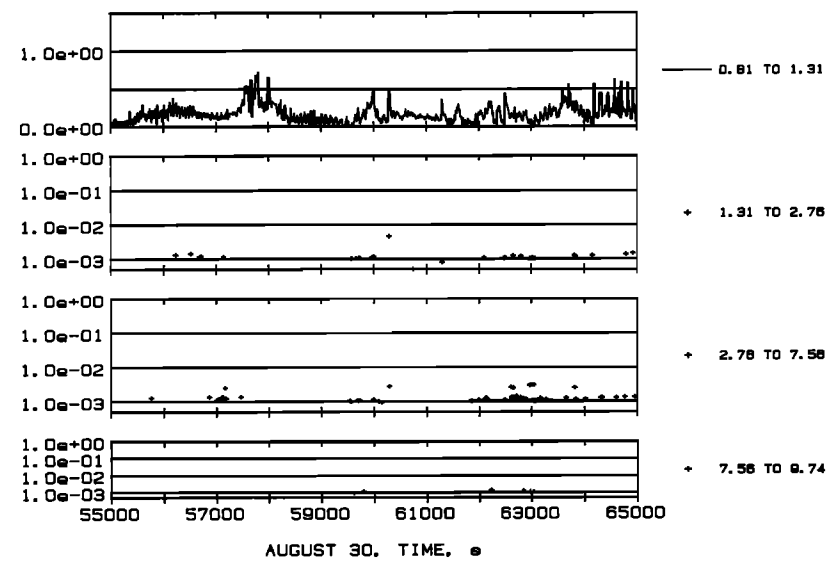

Fig. 13. Fraction of total particles measured in each size range on August 30. The bottom three curves are shown with a log scale. From top to bottom the diameter ranges are 0.81–1.31, 1.31–2.76, 2.76–7.56, and 7.56–9.74 μm.

produced ice crystals from every nucleus when observed FSSP concentrations were used.

Isentropic back trajectories calculated for the 420 K theta surface for August 17 show cooling rates between 10 and 20 K d^{-1} [*McKenna et al.*, this issue]. This cooling occurred as the air moved around the vortex and does not include the effects of mountain waves. Results of calculations modeling the formation of $HNO_3 \cdot 3H_2O$ particles in the Antarctic stratosphere [*Poole and McCormick*, 1988] are applicable to the examples of SD2 observed on August 17. These results show that cooling rates in excess of 2.5 K d^{-1} should cause a large fraction of the nuclei in the background size distribution to nucleate and grow. The model assumed that the growth of particles is limited by mass transfer in the gas phase of the condensing vapor. The air parcel trajectories and aerosol growth models are consistent with these observations of type SD2 distributions.

On August 18 the SD2 type distributions occurred in a region frequently influenced by waves. The fraction grown, however, was less than in the episodes on August 17. On August 30 an even smaller fraction of the nuclei grew in the 0.81- to 1.31-μm-diameter range in the SD2 distributions. Since this air showed evidence of denitrification, less NO_y was available.

The third type of size distribution, SD3, contained particles larger than 2.76 μm. The composition of these particles is unknown.

The model of *Poole and McCormick* [1988] was able to produce large $HNO_3 \cdot 3H_2O$ particles by nucleating less than 5% of the available nuclei with cooling rates of the order of tenths of degrees per day. At those rates, diffusion of vapor to the growing particles depletes the vapor fast enough to keep the supersaturation from reaching levels required to activate the small particles. The model probably requires a nucleation barrier in order to simulate situations in which the fraction of particles growing to large sizes was much smaller than 5% (L. Poole, personal communication, 1989). The observations of SD3 on August 18 were made while encountering mountain waves. Rapid oscillations in temperatures are expected in this region. Parcels of air following θ surfaces probably experienced temperature swings of ± 2°C with a period of about 5 min. The response of these aerosol systems to this type of forcing is unknown. Monotonic, slow cooling does not seem likely. So both the composition and formation mechanism of the large particles in the SD3 size distributions are unknown.

In the cases of SD1 and SD2, large fractions of the sulfate aerosol were involved in cloud formation. The SD1 particles probably did not settle significantly under gravity, since they probably evaporated upon exiting the mountain wave in which they were formed. If they were to settle significantly under gravity, they would remove a significant fraction of the CN with them. Similarly, if the nitric acid trihydrate particles in SD2 were to be incorporated into large ice particles which could settle significantly, the removal of a significant fraction of the NO_y would remove a significant fraction of the sulfate nuclei. Comparisons of the CN-N_2O relationship in and out of denitrified air suggest that this did not routinely happen.

In order to remove NO_y and water from the chemically perturbed region without destroying the CN-N_2O relationship, a mechanism for getting these species onto a few large particles is needed. The observations considered here fail to reveal a clear microphysical path by which this can occur.

CONCLUSIONS

The vertical profile of the CN mixing ratio was found to be closely related to that of N_2O. The location of the minima in the CN mixing ratio profile between -71° and -53° latitude was near the 160 ppbv N_2O isopleth. This observation and others suggest that the processes of mixing and subsidence which determine the inclination of that isopleth also strongly affected the spatial distribution of the sulfate aerosol.

New particle production was observed in air above and south of the 160 ppbv N_2O isopleth. This close relationship between the region of particle production and the dynamic tracer N_2O suggests that the production mechanism may be related to the amount of subsidence but does not exclude a chemical origin.

Similar CN mixing ratios were found in denitrified air and nondenitrified air with similar N_2O mixing ratios. This suggests that a minority of the nuclei were removed in denitrification events or that they were replaced by aerosol production processes.

Comparison of CN concentration with concentrations of particles larger than 0.81 μm provides a means of comparing observations of polar stratospheric cloud events with models of PSC formation. Known events of rapid cooling produced clouds with compositions and properties in agreement with published theories. But these types of clouds may not have contributed to removal of NO_y and water from the CPR. Size distributions were observed in which a few particles reached a large enough size to sediment but their composition was unknown.

Acknowledgments. In support of this work, J. M. Piasecki did computer programming in the field, and Wei Xu did data analysis after the AAOE missions. The spirit of cooperation among participants in AAOE was splendid and inspiring. Gathering of these data required dedication and courage on the part of the people who maintain and fly the ER-2 aircraft. Particularly useful conversations were held with Lamont Poole, Mark Stolzenburg, and Susan Solomon. This work was funded by NASA grant NAG 2-458 through the Atmospheric Experiments Branch, NASA Ames Research Center.

REFERENCES

Arnold, F. A., R. Fabian, and W. Joos, Measurements of the height variation of sulfuric acid vapor concentration in the stratosphere, *Geophys. Res. Lett.*, *8*, 293–296, 1981.

Baumgardner, D., J. E. Dye, and B. W. Gandrud, Calibration of the forward scattering spectrometer probe used on the ER-2 during the AAOE, *J. Geophys. Res.*, this issue.

Chan, K. R., S. G. Scott, T. P. Bui, S. W. Bowen, and J. Day, Temperature and horizontal wind measurements on the ER-2 aircraft during the 1987 Airborne Antarctic Ozone Experiment, *J. Geophys. Res.*, *94*, 11,573–11,587, 1989.

Chen, Y. S., and C. S. Wang, Motion of particles in bends in circular pipes, *Atmos. Environ.*, *15*, 301, 1981.

Crutzen, P. J., and F. Arnold, Nitric acid cloud formation in the cold Antarctic stratosphere: A major cause for the springtime "ozone hole," *Nature*, *324*, 651, 1986.

DeMore, W. B., M. J. Molina, S. P. Sander, D. M. Golden, R. F. Hampson, J. J. Kurylo, C. J. Howard, and A. R. Ravishankara, Chemical kinetics and photochemical data for use in stratospheric modeling, Evaluation number 8, *JPL Publ.*, *87-41*, 1987.

Denning, R. F., S. L. Guidero, G. S. Parks, and B. L. Gary,

Instrument description of the airborne microwave temperature profiler, *J. Geophys. Res.*, this issue.

Fahey, D. W., K. K. Kelly, G. V. Ferry, L. R. Poole, J. C. Wilson, D. M. Murphy, M. Loewenstein, and K. R. Chan, In situ measurements of total reactive nitrogen, total water, and aerosols in a polar stratospheric cloud in the Antarctic, *J. Geophys. Res.*, *94*, 11,299–11,315, 1989.

Fahey, D. W., D. M. Murphy, C. S. Eubank, K. Kelly, M. H. Proffitt, G. V. Ferry, M. K. W. Ko, M. Loewenstein, and K. R. Chan, Measurements of nitric oxide and total reactive nitrogen in the Antarctic stratosphere: observations and chemical implications, *J. Geophys. Res.*, this issue.

Ferry, G. V., E. Neish, M. Schultz, and R. F. Pueschel, Concentrations and size distributions of Antarctic stratospheric aerosols, *J. Geophys. Res.*, this issue.

Fuchs, N. A., *The Mechanics of Aerosols*, p. 204, Pergamon, New York, 1964.

Gandrud, B. W., P. D. Sperry, L. Sanford, K. K. Kelly, G. V. Ferry, and K. R. Chan, Filter measurement results from the Airborne Antarctic Ozone Experiment, *J. Geophys. Res.*, *94*, 11,285–11,297, 1989.

Gary, B. L., Observational results using the microwave temperature profiler during the Airborne Antarctic Ozone Experiment, *J. Geophys. Res.*, *94*, 11,223–11,231, 1989.

Hanson, D., and K. Mauersberger, Laboratory studies of the nitric acid trihydrate: Implications for the south polar stratosphere, *Geophys. Res. Lett.*, *15*, 855–858, 1988.

Hofmann, D. J., and J. M. Rosen, Stratospheric aerosols and condensation nuclei enhancements following the eruption of Alaid in April 1981, *Geophys. Res. Lett.*, *8*, 1231, 1981.

Hofmann, D. J., J. M. Rosen, and W. Gringel, Delayed production of sulfuric acid condensation nuclei in the polar stratosphere from El Chichon volcanic vapors, *J. Geophys. Res.*, *90*, 2341, 1985.

Hofmann, D. J., J. M. Rosen, and J. W. Harder, Aerosol measurements in the winter/spring Antarctic stratosphere, 1, Correlative measurements with ozone, *J. Geophys. Res.*, *93*, 665, 1988.

Hofmann, D. J., J. M. Rosen, J. W. Harder, and J. V. Hereford, Balloon-borne measurements of aerosol, condensation nuclei, and cloud particles in the stratosphere at McMurdo station, Antarctica, during the spring of 1987, *J. Geophys. Res.*, *94*, 11,253–11,269, 1989.

Kelly, K. K., et al., Dehydration in the lower Antarctic stratosphere during late winter and early spring 1987, *J. Geophys. Res.*, *94*, 11,317–11,357, 1989.

Loewenstein, M., J. R. Podolske, K. R. Chan, and S. E. Strahan, Nitrous oxide as a dynamical tracer in the 1987 Airborne Antarctic Ozone Experiment, *J. Geophys. Res.*, *94*, 11,589–11,598, 1989.

McCormick, M. P., C. R. Trepte, and M. C. Pitts, Persistence of polar stratospheric clouds in the southern polar region, *J. Geophys. Res.*, *94*, 11,241–11,251, 1989.

McElroy, M. B., R. J. Salawitch, and S. C. Wofsy, Antarctic O_3: Chemical mechanisms for the spring decrease, *Geophys. Res. Lett.*, *13*, 1296, 1986.

McKeen, S. A., S. C. Liu, and C. S. Kiang, On the chemistry of stratospheric SO_2 from volcanic eruptions, *J. Geophys. Res.*, *89*, 4873, 1984.

McKenna, D. S., R. L. Jones, A. T. Buckland, J. Austin, A. F. Tuck, R. H. Winkler, and K. R. Chan, The southern hemisphere lower stratosphere during August and September 1987: Analyses based on the United Kingdom Meteorological Office Global Model, *J. Geophys. Res.*, this issue.

Molina, M. J., T. L. Tso, L. T. Molina, and F. C. Y. Wang, Antarctic stratospheric chemistry of chlorine nitrate, hydrogen chloride, and ice: Release of active chlorine, *Science*, *238*, 1253, 1987.

Oppenheimer, M., Stratospheric sulfate production and the photochemistry of the Antarctic circumpolar vortex, *Nature*, *328*, 702, 1987.

Podolske, J. R., M. Loewenstein, S. E. Strahan, and K. R. Chan, Stratospheric nitrous oxide in the southern hemisphere, *J. Geophys. Res.*, this issue.

Poole, L. R., and M. P. McCormick, Polar stratospheric clouds and the Antarctic ozone hole, *J. Geophys. Res.*, *93*, 8423–8430, 1988.

Proffitt, M. H., et al., A chemical definition of the boundary of the Antarctic ozone hole, *J. Geophys. Res.*, *94*, 11,437–11,448, 1989.

Pueschel, R. F., K. G. Snetsinger, J. K. Goodman, O. B. Toon, G. V. Ferry, V. R. Oberbeck, J. M. Livingston, S. Verma, W. Fong, W. L. Starr, and R. K. Chan, Condensed nitrate, sulfate, and chloride in Antarctic stratospheric aerosols, *J. Geophys. Res.*, *94*, 11,271–11,284, 1989.

Pui, D. Y. H., F. Romay-Novas, and B. Y. H. Liu, Experimental study of particle deposition in bends of circular cross section, *Aerosol Sci. Technol.*, *7*, 301, 1987.

Rader, D. J., and V. A. Marple, The effects of anisokinetic sampling, *Aerosol Sci. Technol.*, *8*, 283–299, 1988.

Solomon, S., The mystery of the Antarctic ozone hole, *Rev. Geophys.*, *26*, 131, 1988.

Stolzenburg, M. R., and P. H. McMurry, Counting efficiency of an ultrafine aerosol condensation nucleus counter: Theory and experiment, in *Aerosols: Formation and Reactivity*, p. 786, Pergamon, New York, 1986.

Tolbert, M. A., M. J. Rossi, R. Malhotra, and D. M. Golden, Reaction of chlorine nitrate with hydrogen chloride and water at Antarctic stratospheric temperatures, *Science*, *238*, 1258, 1987.

Toon, O. B., P. Hamill, R. P. Turco, and J. Pinto, Condensation of HNO_3 and HCl in the winter polar stratosphere, *Geophys. Res. Lett.*, *13*, 1284, 1986.

Toon, O. B., R. P. Turco, J. Jordan, J. Goodman, and G. V. Ferry, Physical processes in polar stratospheric ice clouds, *J. Geophys. Res.*, *94*, 11,359–11,380, 1989.

Tuck, A. F., R. T. Watson, E. P. Condon, J. J. Margitan, and O. B. Toon, The planning and execution of ER-2 and DC-8 aircraft flights over Antarctica, August and September 1987, *J. Geophys. Res.*, *94*, 11,181–11,222, 1989.

Turco, R. P., R. C. Whitten, and O. B. Toon, Stratospheric aerosols: Observation and theory, *Rev. Geophys.*, *20*, 233–279, 1982.

Wilson, J. C., J. H. Hyun, and E. D. Blackshear, The function and response of an improved stratospheric condensation nucleus counter, *J. Geophys. Res.*, *88*, 6781, 1983*a*.

Wilson, J. C., E. D. Blackshear, and J. H. Hyun, Changes in the sub-2.5 micron diameter aerosol observed at 20 km altitude after the eruption of El Chichon, *Geophys. Res. Lett.*, *10*, 1029, 1983*b*.

K. R. Chan, G. V. Ferry, and M. Loewenstein, NASA Ames Research Center, Moffett Field, CA 94035.

D. W. Fahey and K. K. Kelly, Aeronomy Laboratory, National Oceanic and Atmospheric Administration, 325 Broadway, Boulder, CO 80303.

B. Gary, Jet Propulsion Laboratory, 4800 Oak Grove Drive, Pasadena, CA 91109.

S. D. Smith, Dillon Smith Engineering, Inc., 1457 Idaho Avenue S., St. Louis Park, MN 55426.

J. C. Wilson, Department of Engineering, University of Denver, Denver CO 80208.

(Received August 10, 1988;
revised June 2, 1989;
accepted June 2, 1989.)